ECN test farm measurements for validation of wake models

L.A.H. Machielse, P.J. Eecen, H. Korterink, S.P. van der Pijl, J.G. Schepers,
ECN
machielse@ecn.nl

Abstract

Measurement results are presented from the EWTW test farm of ECN consisting of five 2.5 MW turbines in a row and a meteorological measurement mast of 108 m height. The data cover a period of about 2 years and are gathered for the validation of models for wake simulation and farm design.
The results presented in this paper comprise:

- farm performance for wind directions at small angles with the row,
- performance of the individual turbines in the row up to quadruple wake conditions,
- performance of a turbine in single wake conditions at regular and double rotor distance (3.8*D* and 7.6*D*),
- turbulence intensities and turbulence ratios in single wakes at 2.5*D* and 3.5*D* distance behind the rotor.

The results show that with wind directions at angles of about 25° with the farm orientation the leeward turbines produce more power than the 1st turbine and that the difference increases downwind up to 14%.
Striking and unexpected results are similar maximum performance deficits in single wakes at 3.8*D* and 7.6*D* and very low turbulence intensities and a "hat shaped" velocity profile in the single wake at 2.5*D*.

The measured wind velocity profiles in the wake have been compared with preliminary numerical simulations of ECN's WAKEFARM program. This program can be characterised as a parabolised k-ε turbulence model. A well known problem of such parabolised wake codes is that they commonly account the near wake by means of a very uncertain empirical initialisation. The present model accounts the near wake through results from a physical model.
The width of the wake was very well predicted and fair agreement with the magnitude of the velocity deficit was observed. The turbulence in the wake directly behind the rotor is not well predicted.

1. Test farm

The test farm is part of the ECN Wind turbine Test station Wieringermeer (EWTW). The station is located in the Netherlands, 35 km northeast of the ECN premises in flat open farmland. The centre of the farm is about 1200 m from the dike along a vast lake, the IJsselmeer. The distance to the other part of the test station - a row of test locations for prototype turbines - is about 1600 m (Fig. 1)

The farm consists of a row of 5 state of the art turbines of 2.5 MW and a meteorological measurement mast. The variable speed, pitch controlled turbines have rotor diameters and hub heights of 80 m. Rated wind speed is approximately 15 m/s. The rotor speed varies between 10.9 and 19.1 RPM.

The spacing between the turbines is 3.8 rotor diameters (305 m). The orientation of the row is 95º with respect to north. The turbines are numbered from 5 to 9, with the most westward turbine as number 5 (T5). Fig. 2 gives the distances and directions from the mast to the individual turbines.

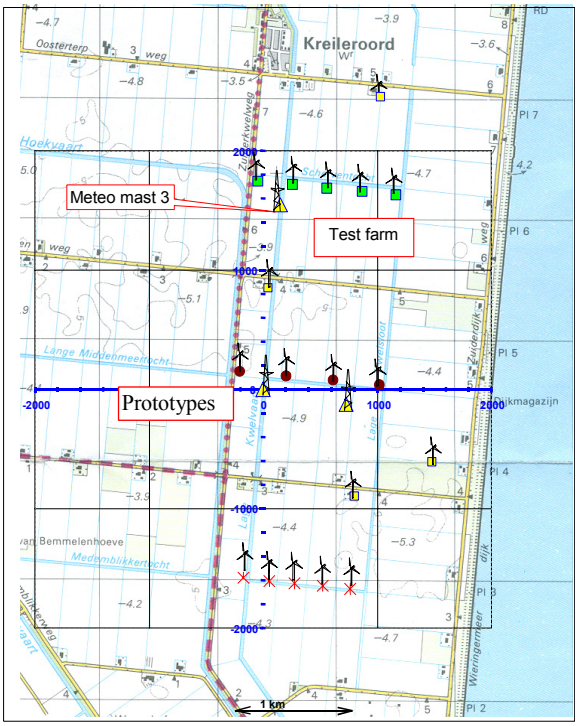

Fig. 1 Map of the test station with test farm, prototypes, measurement masts and surrounding obstacles

The 3-year averaged wind speed at the location is 7 m/s at 71.6 m height [1]. Prevailing wind directions are from southwest to northwest.

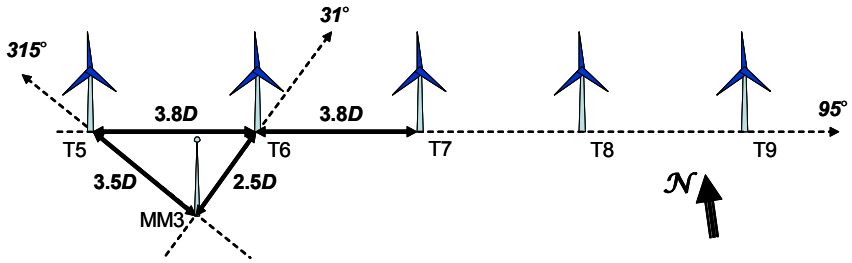

Fig. 2 Main dimensions and directions of the test farm

2. Data-acquisition

The test farm is provided with extended means for automatic acquisition and storage of meteorological data, operational parameters of all turbines, bending moments in the blade roots and tower base of T6 and of numerous condition monitoring data and other data for specific experiments.

Calibration of sensors and measurement chains and various types of data validation – automatically by the measurement hardware and carried out by experts - ensure a high quality level.
The data acquisition system, database and data validation is described by Eecen et al. [2].

Meteorological data

The meteorological data are measured in measurement mast MM3 at the south side of the test farm. This is a guyed, lattice tower with a triangular cross section and measurement booms pointing in north, southwest and southeast directions.

Wind measurement equipment is installed at hub height (80 m) and about 70% of the rotor radius above and below hub height. The disturbance of the wind speed and wind direction for a similar tower at the test station has been measured and is less than 1%.

The instrumentation of MM3 consists of (Fig. 3):

- sonic anemometers at 52 and 80 m height on the north booms and on the top of the tower (109.1 m),
- cup anemometers and vanes at the south-east and south-west booms at 52 and 80 m height,
- sensors for ambient temperature, pressure and humidity at 78.4 m height,
- sensor for the temperature difference between 37 and 10 m height.

The wind characteristics in the wake presented in this paper are measured with the sonic anemometer at hub height. This instrument is mounted on the north boom that points towards the farm and therefore is very well suited for wake measurements.

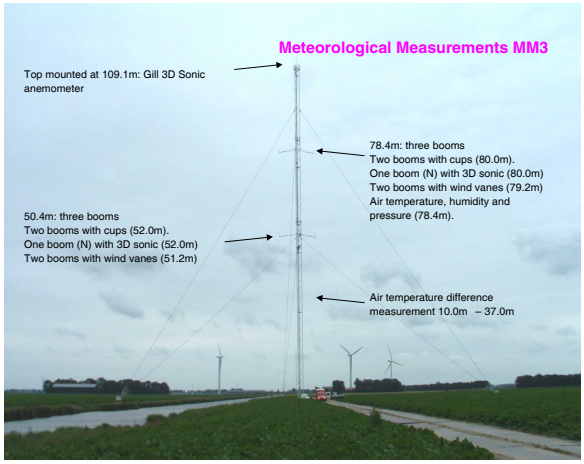

Fig 3. Measurement instruments and their locations in mast MM3.

Operational data

For each turbine, the data acquisition system measures the produced power, the generator speed, the wind speed and direction measured at the nacelle, the pitch angles of the blades, the yaw angle and the operation code.
Some of these parameters have been used for the selection of records with continuous normal operation of the turbines.

3. Data processing

This paper only presents 10-minute averaged data, their standard deviations and derived quantities.

Measured power values (P_{farm} or P_i for individual turbines) are not corrected for ambient temperature and pressure.

Presented wind data in the wake are measured with the sonic anemometer at 80 m on the north boom. The velocity components in the main flow direction and the lateral and vertical direction are denoted by *u, v* and *w*. respectively.

Ambient conditions

MM3 has a fixed position. Therefore, simultaneous measurement of the ambient conditions (wind velocity, wind direction and turbulence intensity) is not possible when the mast is standing in the wake of one of the turbines. Yet, these conditions are needed for classification of the results.

As T5 is freely exposed to the considered wind directions, the ambient wind speed is estimated from its nacelle wind speed V_{nac} and the ambient wind direction from its nacelle direction θ_{yaw}. The ambient wind speed is denoted by V' and the ambient direction by θ'.

The transfer functions have been determined from undisturbed wind direction sectors from records with T5 continuously in normal operation but without further distinction for conditions like average wind speed, turbulence intensity or atmospheric stability.
The applied fitting relations are:

$$V' = 0.0131 \cdot V_{nac} \text{ ^ } 2 + 0.7355 \cdot V_{nac} + 1.3133$$
$$\theta' = \theta_{yaw} + 9.58$$

Mostly, the results are presented for different intervals of ambient wind speed (2 m/s wide), turbulence intensity (2%) and wind direction (2°).
The direction profiles in this paper have been smoothened by weighted averaging across 3 bins with a weighing factor of 50% for the outside bins. Only small deviations occur from this approach. E.g. the average relative velocity in the wake in a single bin of 2° wide does not differ more than 4% from the weighted value. The standard deviation of the difference is less than 1.5%.

Fig. 4. shows the turbulence intensity $\sigma(u)/u$ for the undisturbed sector southwest of the farm (245° to 275°). The turbulence intensities at higher wind speeds are consistent with flat open farmland.

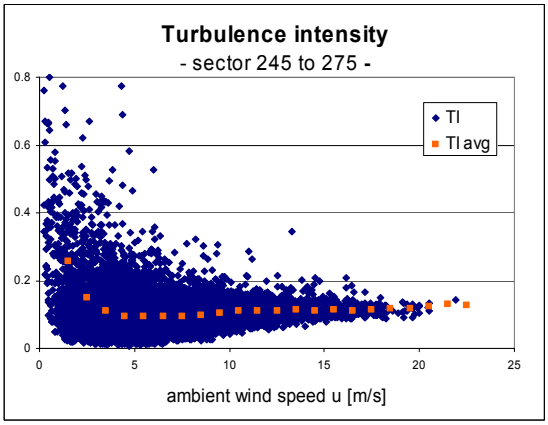

Fig. 4 Turbulence intensity $\sigma(u)/u$ at hub height measured in the undisturbed sector from 245° to 275°.

Direct measurement of the incoming turbulence intensity $\sigma(u)/u$ was not possible with MM3 in the wake and no other mast upwind of the turbine. Therefore the turbulence intensity is related to the ambient wind speed V' in this paper.
The deviation between both values has been determined for the undisturbed wind sector from 245° to 275°. For ambient wind speeds of 4 to 20 m/s the relative difference between the average values of $\sigma(u)/u$ and $\sigma(u)/V'$ is less than 2%.

4. Farm performance

This section presents performance data of the farm in wind directions at small angles with the farm orientation, so when the turbines are influenced by each other's wake.

Only data from prevailing westerly wind directions have been selected. In these directions, the first turbine in the row (T5) will not be influenced by the wake. Therefore its performance is used as reference for the undisturbed performance of the farm. The relative farm performance is given by:

$$P_{rel} = \Sigma P_i / (5 \cdot P_5) \text{ with } (i = 5, \ldots, 9)$$

The measuring mast MM3 is not influenced by the wake when the wind is blowing at small angles with the farm from southwest directions. This is shown in Fig. 5. The figure gives the horizontal profile of the average turbulence intensity $\sigma(u)/V'$. Up to directions of about 15º with the farm axis the average turbulence intensity does not increase. Thus, up to this limit classification for different turbulence intensity classes is possible.

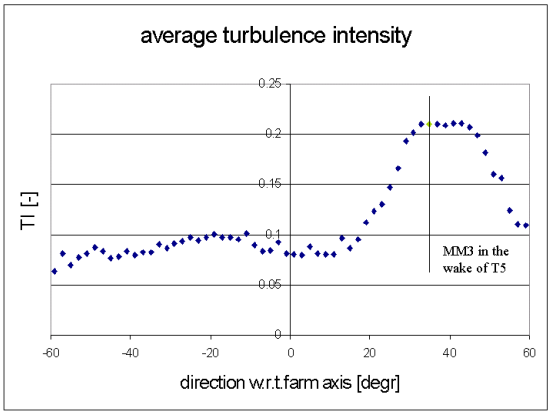

Fig. 5 Average turbulence intensity from wind directions at small angles with the farm orientation.

Fig. 6 and Fig. 7 give the relative farm performance for average ambient wind speeds V'

from 4 to 14 m/s and for 3 ambient turbulence intensity classes *σ(u)/V'* up to 15%.
As can be seen, production is reduced for wind directions across a sector of about 45º wide. The relative performance drops to about 45% in the centre of the wake sector at low wind speeds and turbulence intensities.

Furthermore, Fig. 6 and Fig. 7 show that for the particular farm configuration the wake sector consists of different parts: a core where the relative performance is dominated by the ambient conditions that is flanked by small sectors where the ambient conditions hardly have any influence. Overall, the full width of the wake sector is hardly influenced by the conditions.

The results seem convincing considering the high number of 10-minute averages in the population (6669 in the sector from -33° to 33°) and the small variation in standard deviation (Fig. 8)

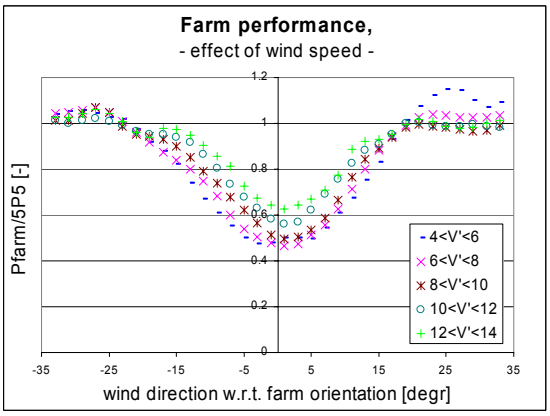

Fig. 6 Relative farm performance as function of the wind direction w.r.t. the farm orientation for different classes of ambient wind speed *V'*.

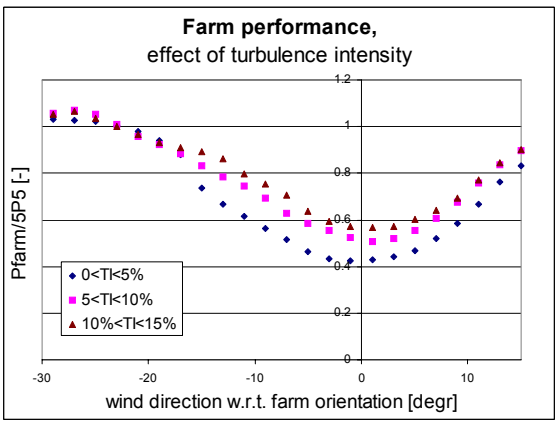

Fig. 7 Relative farm performance as function of the wind direction w.r.t. the farm orientation for different classes of turbulence intensity *σ(u)/V'*.

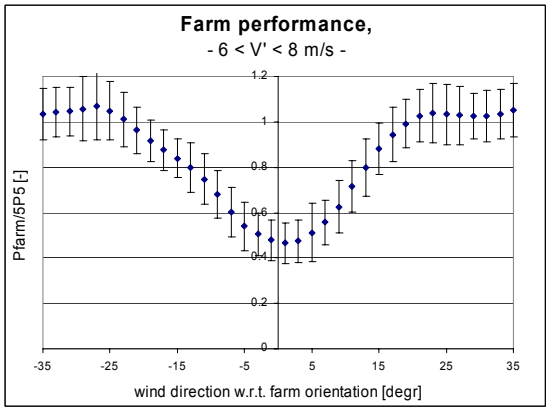

Fig. 8 Relative farm performance with standard deviation for 6<V'<8 m/s.

Figures 9 and 10 show the averages and the minima of the relative farm performances in the wake sector. The values are determined from the data presented in figures 6 and 7 across a 44° degrees wide sector centred in the hart of the wake.

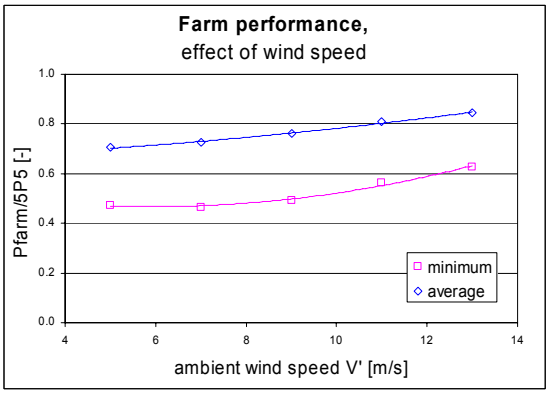

Fig. 9 Minimum and average farm performance depending on wind speed. Average determined from figure 6 from a 44° degrees wide centred part of the wake sector.

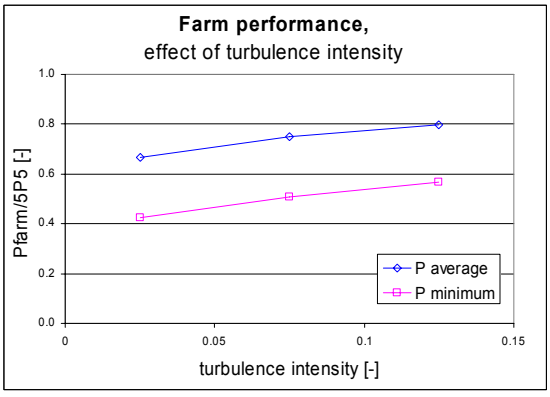

Fig. 10 Minimum and average farm performance depending on turbulence intensity. Average determined from figure 7 from a 44° degrees wide centred part of the wake sector.

The average performance is lowest at low wind speeds (70% of the free flow performance). The average performance gradually increases with increasing wind speed to 85% at 13 m/s.

The average performance for turbulence intensities from 0% to 5% (68%) is about 12% lower than the average for intensities from 10% to 15%.

5. Turbine performance

This section presents the performance of the individual turbines in westerly wind directions at small angles with the farm orientation. The performance is made dimensionless with the performance of T5 that is not influenced by the wake in these directions.
The relative performance of turbine $P_{i,rel}$ is given by:

$P_{i,rel} = Pi/P_5$ with i = 6,..,9

As an example, Fig. 11 shows the horizontal profile for the relative performances of the turbines 6 to 9 for ambient wind speeds V' of 6 to 8 m/s.
The figure shows a typical phenomenon that is observed in other wind speed classes too. Adjacent to the wake sector the leeward turbines produce more power than T5. The surplus increases from the front to the end of the row, thus from T6 to T9.
The performance of T9 at an average wind speed of 7 m/s is 14% higher than that of T5. The difference decreases to 9% at 13 m/s.

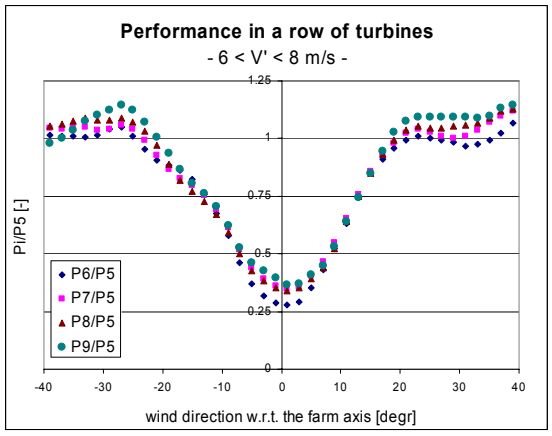

Fig.11 Relative performance of the wind turbines T6 to T9 for wind speed interval $6<V'<8$ m/s. The figure is made up of 3288 10-minute averages. The lowest number of data points in one bin is 45.

Fig. 12 shows the average values for the relative performance with standard deviations in the bin with the highest value of $P_{9,rel}$ ($-28°<\theta'<-26°$) and ambient wind speed $6<V'<8$ m/s. Both the average value and the standard deviation increase in flow direction. This phenomenon should be investigated further.

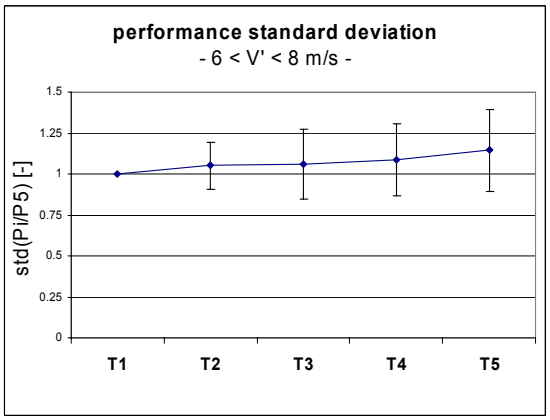

Fig. 12 Average performance and deviation in bin $-28°<\theta'<-26°$ for $6<V'<8$ m/s. The bin contains 83 10-minute averages.

The minima of the relative performances across the wake sector are presented in Figures 13 and 14, respectively for different classes of ambient wind speed V' and turbulence intensity $\sigma(u)/V'$.

The differences in relative performance between the turbines T7 to T9 are very small at low ambient wind speeds and disappear at increasing wind speed.
At low wind speeds the 2nd turbine of the row (T6) clearly produces the least power in the centre of the wake. This changes with increasing wind speed. As a result the performance of T6 becomes higher than that of T7, T8 and T9 above $V' = 11$ m/s.

The relative performances of the three last turbines are almost the same for all turbulence intensities. Only at low turbulence intensity levels, the minimum performance of T6 in the centre of the wake is significantly lower than the performance of the other turbines.

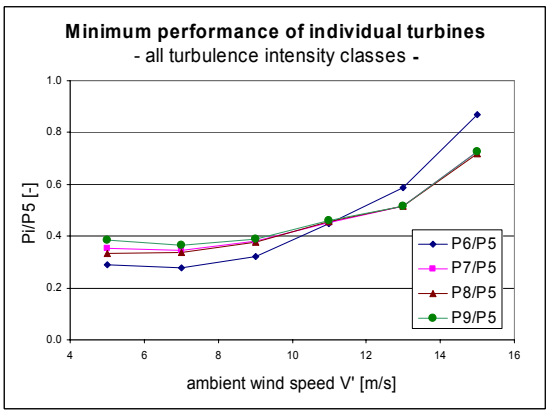

Fig.13 Relative performance minima of the wind turbines T6 to T9 in the wake depending on ambient wind speed V'.

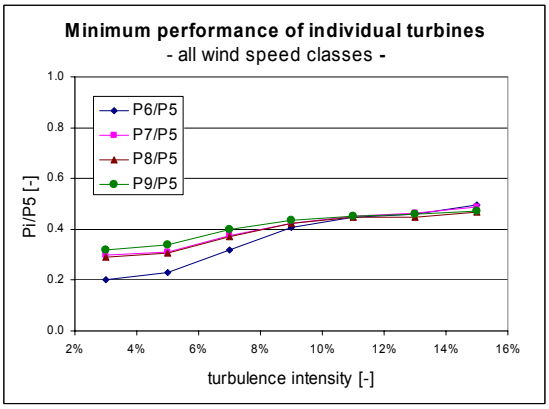

Fig.14 Relative performance minima of the wind turbines T6 to T9 in the wake depending on ambient turbulence intensity $\sigma(u)/V'$.

6. Performance at double distance

The turbines in the test farm are placed at a distance of 3.8*D*. So, when turbine 6 is standing still, turbine 7 becomes the 2nd operating turbine in the row at a distance of 7.6*D*. Enough records have been gathered for an impression of the effect.

Fig. 15 compares the minimum performance of the 2nd turbine at both distances depending on the ambient wind speed and for all turbulence intensity classes. The minimum performance clearly is increased at 7.6*D*.

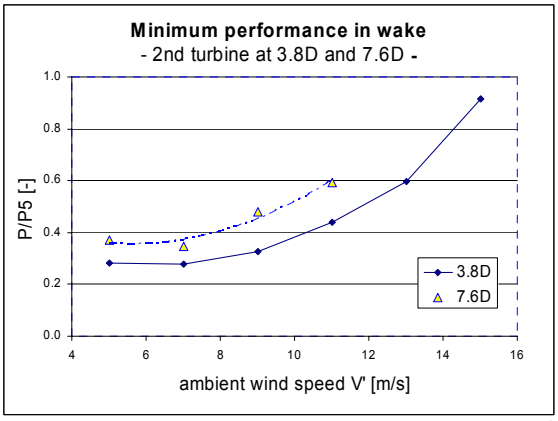

Fig.15 Relative performance minima of the 2nd wind turbine at 3.8*D* and 7.6*D* distance as function of ambient wind speed *V'*.

Fig. 16 compares the profiles for the relative performance of the 2nd turbine in the turbulence intensity class 10%<$\sigma(u)/V'$<12%.
Again, it looks like the wake sector consists of a core flanked by small sectors where the ambient conditions have hardly any influence.
Fig. 17 gives the same information but for very low turbulence intensities (2%<$\sigma(u)/V'$<4%). Strikingly, the minimum performance in these conditions is nearly equal for 3.8*D* and 7.6*D* rotor distance.

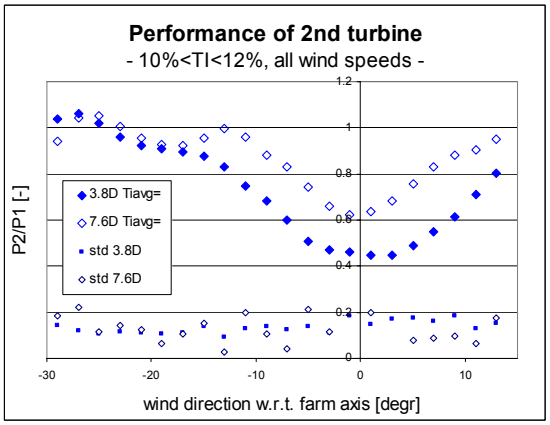

Fig.16 Relative performance profile with standard deviation of the 2nd turbine in the wake at 3.8*D* and 7.6*D* distance for turbulence intensity 10%<$\sigma(u)/V'$<12%.

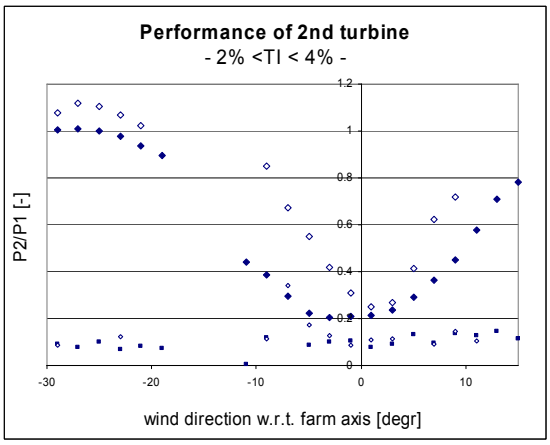

Fig.17 Relative performance profile with standard deviation of the 2nd turbine in the wake for 3.8*D* and 7.6 *D* distance for low turbulence intensity (2%<$\sigma(u)/V'$<4%).

7. Wind velocity in the wake

This section deals with the changes in the average wind velocity in the wake.

The wind speed in the wake is measured at hub height by the sonic anemometer. The average wind direction at that location differs from ambient. But, as the measured average differences are smaller than 4° the expected errors will be less than 1%.

Due to the lay-out of the test farm and the position of measurement mast MM3 complete profiles of the wind characteristics only can be measured for single wake conditions at rotor distances of 2.5*D* and 3.5*D*, respectively behind T6 and T5.

Fig. 18 shows the maximum velocity deficit for distances of 2.5*D* and 3.5*D* behind the rotor and different values of the ambient wind speed.

The velocity deficit V_{def} is:

$$V_{def} = (V'-u)/V'$$

with u as longitudinal wind speed component measured by the sonic anemometer.

The maximum deficit is highest at low wind speeds where the tip speed ratio λ is relatively high and thus the axial force coefficient. The highest deficit is 45% at 2.5D distance behind the rotor and 35% at 3.5D. These tendencies are in agreement with the tendencies in the power measurements in section 5.

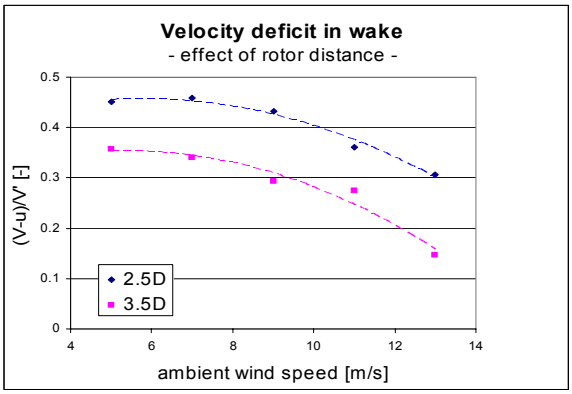

Fig.18 Maximum wind velocity deficit $(V'-u)/V'$ at hub height depending on ambient wind speed V' in single wakes at 2.5D and 3.5D distance behind the rotor.

The horizontal profile of the velocity deficit at 2.5D distance is presented in Fig. 19. The maximum deficit clearly decreases with increasing ambient velocity. The width of the wake sector becomes smaller with increasing velocity.

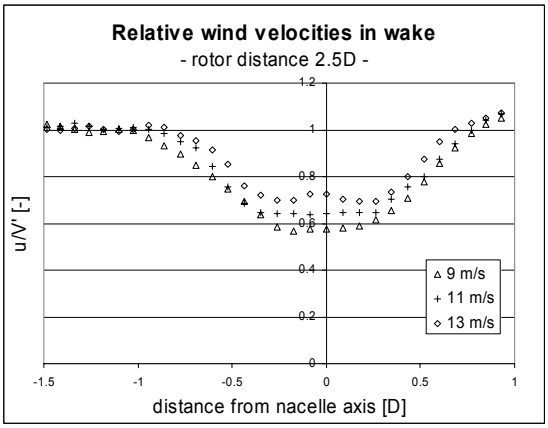

Fig.19 Horizontal wind speed profile in a single wake at 2.5D behind the rotor for 3 ambient wind speed classes of 2 m/s width.

The profile tends to form a horizontal level in the center at this (short) distance behind the rotor. Opposite to the expectations by Schepers [3] in the ENDOW project (Efficient development of offshore wind farms) it looks like the effect of momentum exchange with the outer flow has not reached the central area yet.
Such a clear horizontal level is not observed at 3.5D distance (Fig. 20).

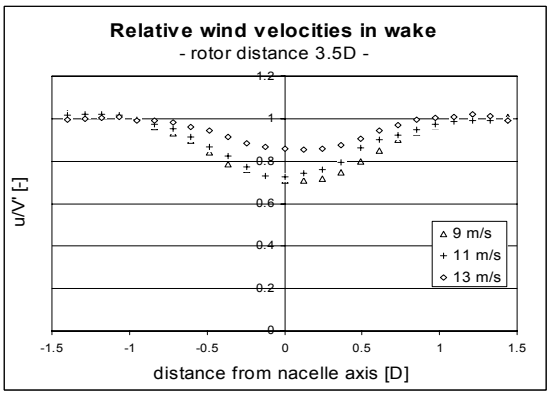

Fig.20 Horizontal wind speed profile in a single wake at 3.5D behind the rotor for 3 ambient wind speed classes of 2 m/s width.

8. Turbulence in the wake

This section presents the turbulence intensity $\sigma(u)/V'$ and the ratios between the standard deviations of the wind speed components in horizontal and vertical directions, respectively $\sigma(v)/\sigma(u)$ and $\sigma(w)/\sigma(u)$.

The turbulence intensity is related to the ambient wind speed V' instead of the average wind speed u at the sensor location for easy assessment of the added turbulence compared to ambient.
Again, no corrections are made to compensate for the difference between the average ambient wind direction and the local wind direction in the wake. The resulting errors are expected to be negligible (see previous section).

The turbulence intensity $\sigma(u)/V'$ at 2.5D and 3.5D for different ambient wind speed intervals are presented in Fig. 21 and Fig. 22. The figures clearly show increased intensity levels in the wake. The ambient intensity is increased with up to about 10%-points. The intensity difference decreases with increasing average wind speed.

In the figures, also the typical shape related to shear production of turbulence can be distinguished with 2 maxima besides the centre.
This certainly is the case at short distance behind the rotor (2.5D) where the local maxima can be distinguished very well. The turbulence intensity in the center of the wake clearly decreases with increasing wind speed. At V' = 13 m/s the turbulence intensity level even becomes comparable with ambient.

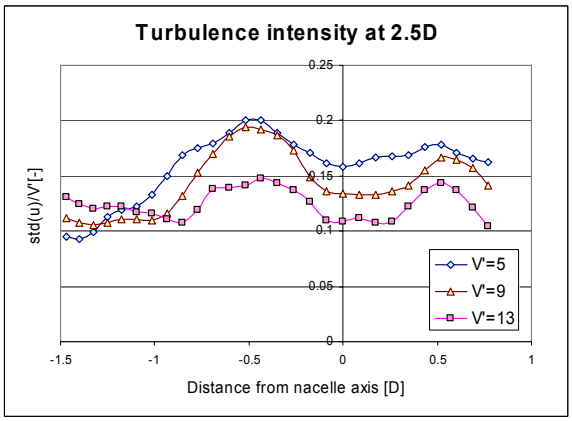

Fig.21 Turbulence intensity $\sigma(u)/V'$ in a single wake at 2.5D behind the rotor for 3 wind speed intervals (width 2 m/s).

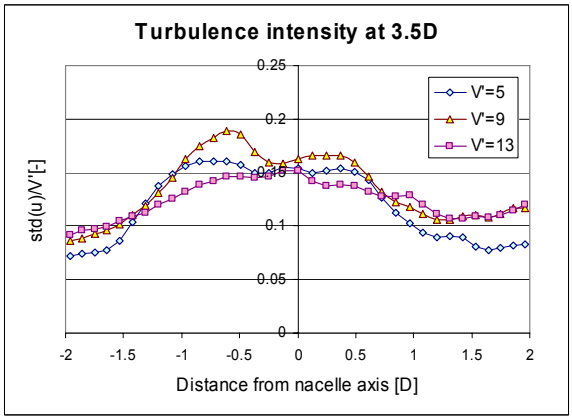

Fig.22 Turbulence intensity $\sigma(u)/V'$ in a single wake at 3.5D behind the rotor for 3 wind speed intervals (width 2 m/s).

Figures 23 and 24 present the turbulence ratios $\sigma(v)/\sigma(u)$ and $\sigma(w)/\sigma(u)$ in lateral and vertical direction for the wind speed interval 6<V'<8 m/s. At both distances the profiles show maxima in the centre of the wake and the difference between both ratios becomes smaller. Further, the lateral turbulence ratios are flanked by local minima.

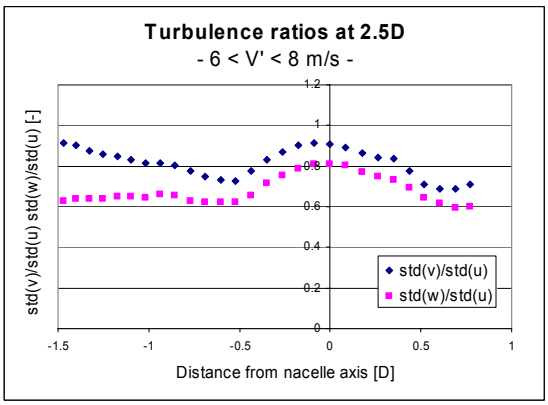

Fig.23 Horizontal profile for the lateral and vertical turbulence ratios, $\sigma(v)/\sigma(u)$ and $\sigma(w)/\sigma(u)$ at 2.5D distance and an average ambient wind speed of $6<V'<8$ m/s.

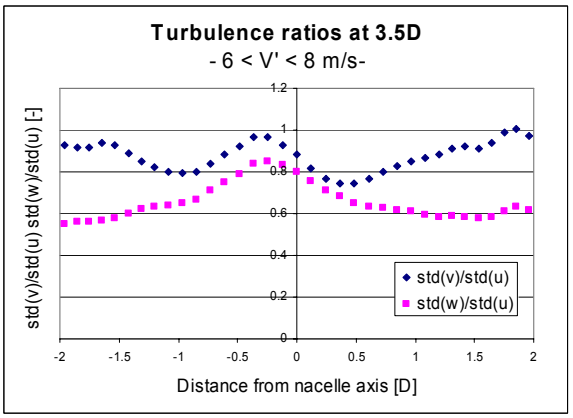

Fig.24 Horizontal profile for the lateral and vertical turbulence ratios, $\sigma(v)/\sigma(u)$ and $\sigma(w)/\sigma(u)$ at 3.5D distance and an average ambient wind speed of $6<V'<8$ m/s.

9. Numerical simulations

The measured velocities in the wake have been compared with preliminary numerical simulations with the WAKEFARM model. The WAKEFARM model is derived from the UPMWAKE model of Crespo et al. [5]. It is based on the parabolised Navier-Stokes equations and incorporates the k-ε turbulence model.

The numerical aspects of the WAKEFARM model are discussed in much detail by Henneman [8].

The WAKEFARM model requires a prescribed incident flow field and thrust coefficient C_T. With this information, it computes the wind speed and turbulence intensity at any location behind the rotor within the computational domain. The C_T curve has a direct influence on the flow field, as it defines the initial velocity deficit in the rotor plane. The difficulty is however, that the rotor thrust is unknown and difficult to measure. Therefore, the thrust coefficient is calculated by a blade element momentum model (BEM).

For the incident flow field the model of Panofsky and Dutton [4] is used, where the velocity and turbulence profiles depend on the roughness height z_0, the Monin-Obukhov length scale l and the friction velocity u^*. These three parameters are not measured directly, but can be determined by fitting the profiles with measured data, see [3] for more details.

For each velocity bin, the bin-average wind speeds at two different heights and bin-average turbulence intensity at hub height have been used to determine the parameters in the Panofsky and Dutton model (Table 2).

u [m/s]	z_0 [m/s]	l [m]	u^* [m/s]
9.15	0.017	365	0.38
11.08	0.018	440	0.48
13.19	0.019	493	0.58

Table 2 Hub-height wind speed u, roughness height z_0, Monin-Obukhov length scale l and friction velocity u^* used as free stream conditions in the calculations.

The parabolisation as applied in the WAKEFARM program is very common for wake codes because it leads to an enormous reduction of calculation effort. The parabolisation is made possible by neglecting the stream wise pressure gradient in the flow equations. This is a fair assumption in the far wake (say for distances > 2D behind the turbine) but not in the near wake. Therefore the near-wake effects were accounted for by an empirical initial velocity profile, applied at the end of the near wake, see Schepers [3]. Similar techniques are used in other wake models, see Barthelmie et al, [10]. More recently a major improvement has been made Van der Pijl and Schepers [6,7]. In their approach the stream wise pressure gradients are not neglected anymore, but they are prescribed, where the prescribed pressure gradients have been calculated with a free wake model for different thrust coefficients. The results are stored into a database and then the WAKEFARM program determines the actual pressure gradient from interpolation. This leads to a very unique wake code since it avoids the common empirical tuning for the near wake where the parabolisation still yields a computational efficient code.

Results

The wake-profiles are presented in Fig. 22. The numerical results are compared with the experimental wake-profiles at 2.5D and 3.5D distance behind the rotor respectively for an average ambient wind speed of 11 m/s.
There is fair agreement between modelling results and experiments, especially at 3.5D. At 2.5D, the WAKEFARM model predicts somewhat smaller velocity deficits than measured.
This might be caused by an overestimation of the turbulence in the wake directly behind the rotor.
It is also interesting that the experimentally observed profile has a nearly constant velocity deficit around the centreline, while the modelled profile is bell-shaped. This also points in the direction of an overestimation of the turbulence directly behind the rotor.
The width of the wake on the other hand is very well predicted.

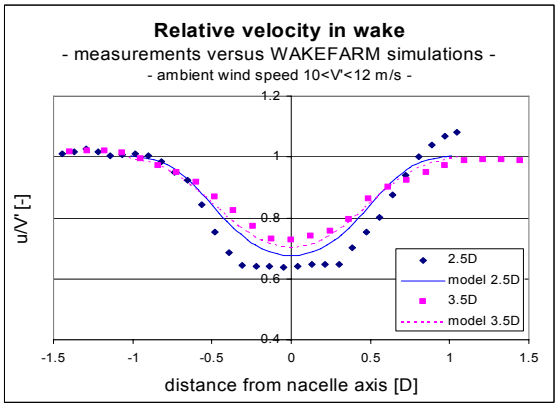

Fig.22 Comparison of model results and experiments for the relative velocity in the wake at distances of 2.5D and 3.5D and an average ambient wind speed $10<V'<12$ m/s.

10. Conclusions

Measurement data have been gathered in the EWTW test farm of ECN during a period of about 2 years for the validation of models for wake simulation and farm design. The data comprise turbine performances in a row of 5 turbines and wind properties (average wind speeds, turbulence intensities and turbulence ratios) in single wakes at 2.5D and 3.5D distance for various conditions of ambient wind speed and turbulence intensity.

The results show that for the particular farm configuration the wake sector consists of a core where the performance is dominated by the ambient conditions flanked by small sectors where the performance is independent of the ambient conditions.
The results also show that with wind directions at angles of about 25° with the farm orientation the leeward turbines produce more power than the 1st turbine and that the difference increases downwind up to 14%.

The wind climate enabled measurements at very low turbulence intensities. Striking and unexpected results in these conditions are similar (maximum) velocity deficits at 3.8D and 7.6D and a "hat shaped" velocity profile at 2.5D.
It was furthermore observed that the turbulence becomes more isotropic in the centre of the wake.

The velocity profile at hub height in the wake at 2.5D and 3.5D distance behind the rotor is compared with preliminary numerical simulations with the WAKEFARM model.
The width of the wake was very well predicted and fair agreement with the magnitude of the velocity deficit was observed.
As there is reason that the turbulence in the wake is not very well predicted directly behind the rotor, it

would be valuable to make a comparison of the modelled and the measured turbulence (intensity) in future research.

Acknowledgement

The activities have been financially supported by the DEN program of the Ministry of Economic Affairs, carried out by SenterNovem.

References

[1] P.J. Eecen and J.P.Verhoef, *EWTW Meteorological database, Description June 2003 -May 2006*, ECN-I--06-004

[2] P.J. Eecen et al. *Measurements at the ECN wind turbine test station Wieringermeer,* European Wind Energy Conference 2006 (EWEC2006), Athens, Greece, 27 February 2006-2 March 2006.

[3] J.G. Schepers, *ENDOW: Validation and improvement of ECN's wake model*, Report ECN-C- 03-0734, ECN, 2003.

[4] H.A. Panofsky and J.A. Dutton, *Atmospheric Turbulence,* Wiley, 1984.

[5] A. Crespo and J. Hernandez, *Numerical modeling of the flow field in a wind turbine wake.* In Proceedings of the 3rd Joint ASCE/ASME Mechanics Conference, pages 121--127. ASME, 1989.

[6] S.P. van der Pijl and J.G. Schepers, *Improvements of the ECN WAKEFARM program,* preprint, 2006.

[7] S.P. van der Pijl and J.G. Schepers, *Improvements of the WAKEFARM wake model,* Presented at the Annex XXIII: Offshore wind energy technology and deployment, Workshop on wake modeling and benchmarking of models, 2006.

[8] B.Henneman, *Numerical aspects of the WAKEFARM program,* Report ECN-C--03-035, ECN, 2003.

[9] S.V. Patankar and D.B. Spalding, *A calculation procedure for heat, mass and momentum transfer in three-dimensional parabolic flows,* International Journal of Heat and Mass Transfer, 15:1787--1806, 1972.

[10] R. Barthelmie et al, *Proceedings of the ENDOW workshop 'Offshore wakes: Measurements and modelling,* RISO, Report. RISO-R1326, March 2002